Arabian Journal of Chemistry 16 (2023) 105241

Contents lists available at ScienceDirect

Arabian Journal of Chemistry

journal homepage: www.sciencedirect.com

Original article

Ligand-based drug design of Pinocembrin derivatives against Monkey-Pox disease

Shopnil Akash [a], Shabana Bibi [b,*], Qudsia Yousafi [c], Awais Ihsan [c], Riaz Mustafa [d], Umar Farooq [e], Atul Kabra [f], Mohammad M. Alanazi [g], Ashwag S. Alanazi [h], Omkulthom Al Kamaly [h]

[a] Faculty of Allied Health Science, Department of Pharmacy, Daffodil International University, Daffodil Smart City, Ashulia, Savar, Dhaka 1207, Bangladesh
[b] Department of Biosciences, Shifa Tameer-e-Millat University, Islamabad 44000, Pakistan
[c] Department of Biosciences, COMSATS University Islamabad Sahiwal Campus, Pakistan
[d] Department of Pathology, University of Agriculture Faisalabad Sub-campus Toba Tek Singh, Pakistan
[e] Department of Poultry Science, University of Agriculture Faisalabad Sub-campus Toba Tek Singh, Pakistan
[f] University Institute of Pharma Science, Chandigarh University, Gharuan, Mohali 140413, Punjab, India
[g] Department of Pharmaceutical Chemistry, College of Pharmacy, King Saud University, P.O. Box 2457, Riyadh 11451, Saudi Arabia
[h] Department of Pharmaceutical Sciences, College of Pharmacy, Princess Nourah bint Abdulrahman University, P.O. Box 84428, Riyadh 11671, Saudi Arabia

ARTICLE INFO

Article history:
Received 6 April 2023
Accepted 3 September 2023
Available online 6 September 2023

Keywords:
Molecular docking
Molecular dynamic simulation
Drug-likeness
ADMET
Pass prediction
Monkey-Pox

ABSTRACT

Severe pathogen infections, such as Monkeypox disease caused by the Monkeypox virus, easily spread in different animals and then into humans. There is an urge for novel therapeutic options, such as medicine/vaccine development to control it. Therefore, we designed Pinocembrin derivatives and performed *in silico* analysis such as molecular docking by PyRx software, molecular dynamics (MD) simulations at 100 ns, binding free energy estimation by AMBER20 software, ADMET profile, and Pass prediction. Optimal results were observed for two derivatives (07 and 11), exhibiting interactions with key residues of the selected protein. These interactions were substantiated by a range of structural and energetic parameters, including binding energies, solvation-free energy models, dynamic fluctuations, hydrogen bonding, and solvent accessibility. Notably, ligands 07 and 11 displayed exceptional binding affinities of −10.3 kcal/mol and −9.6 kcal/mol, respectively. RMSD value presented minor abruptions of about 1.2 to 1.3 Å and superimposed structures of selected derivatives complexes with Monkeypox target protein at 0 ns and 100 ns presented minor fluctuation in the native and bounded conformation. Slight instability is noted from the peaks in graphs of RMSD, RMSF, hydrogen bonds (HBs), beta factor (BF), and solvent-accessible surface area (SASA). Based on promising results, we proposed that Pinocembrin derivatives may serve as novel therapeutic agents against Monkeypox infections. Therefore, strongly advocate for further experimental validation through chemical laboratory testing. Such endeavors could pave the way for the development of effective treatments to mitigate the impact of Monkey-Pox disease.

1. Introduction

Viruses are constantly the major cause of a significant number of newly developing and re-emerging illnesses and become major health concerns for humans and animals (Mourya, 2019). In the developing world, they represent a much bigger problem worldwide especially in terms of public health now than significantly in recent century (Howard and Fletcher, 2012). Most deadly and fatal human illnesses are caused by pathogenic viral infections, which propagate and are a substantial contributor to the worldwide burden of morbidity and death (Jones, 2008). Recently, a life-threatening virus has been spreading globally, infecting numerous people and causing moderate respiratory illness

* Corresponding author at: Department of Biosciences, Shifa Tameer-e-Millat University, Islamabad 44000, Pakistan.
E-mail addresses: shopnil.ph@gmail.com (S. Akash), shabana.bibi.stmu@gmail.com (S. Bibi), qudsia@cuisahiwal.edu.pk (Q. Yousafi), awais@cuisahiwal.edu.pk (A. Ihsan), drriaz@uaf.edu.pk (R. Mustafa), u.farooq@uaf.edu.pk (U. Farooq), atul.kbr@gmail.com (A. Kabra), mmalanazi@ksu.edu.sa (M.M. Alanazi), asalanzi@pnu.edu.sa (A.S. Alanazi), omalkmali@pnu.edu.sa (O. Al Kamaly).

Peer review under responsibility of King Saud University.

Production and hosting by Elsevier

https://doi.org/10.1016/j.arabjc.2023.105241
1878-5352/

(Boopathi et al., 2020). Notable pathogenic viruses include the Monkeypox virus (Mahase, 2022), and the Ebola virus (Malvy, 2019). SARS CoV-2 (Ciotti, 2020), HIV (Hoffmann, 2022), Smallpox (Billioux et al., 2022), Hantavirus (Vaheri, 2013), Influenza (Hutchinson, 2018), Dengue (Ross, 2010), and Langya henipavirus (Akash et al., 2022).

After COVID-19, Monkeypox is another life-threatening viral infection but very rare and has a resemblance to Smallpox. Monkeypox virus belongs to the Poxviridae family, *Chordo-poxvirinae* subfamily, and *Orthopoxvirus genus* (Frenkel and Bellanti, 2022). Since the elimination of Smallpox in 1980, this virus has emerged as the most significant orthopox virus threat to human communities (Sklenovska and Van Ranst, 2018). The term Monkeypox originated in 1958 when the virus was first invented in Monkeys in a Danish research laboratory (von Magnus et al., 1959). But, the first prevalence was announced publically in Congo (in 1970) in a nine-month-old baby boy (Hutson, 2015). Since then, Monkeypox seems to have become widespread in Congo, and it has also expanded to other nations in Africa, mostly those located in Central and West Africa the first cases of Monkeypox to be documented beyond Africa happened in the year 2003 (Sale et al., 2006).

The pathogenic and pathophysiological Monkeypox viral infection has become strongly transmitted among people. On May 13, 2022, the World Health Organization (WHO) announced about three instances of Monkeypox in the United Kingdom, two of which were confirmed in a laboratory and one of which was considered likely (https://www.who.int/). After that, this pathogenic infection spread rapidly from country to country (Mauldin, 2022). The Monkeypox virus is moderately transmissible to humans and may be spread by droplets or close communication with wounds that are affected by the disease (Thornhill, 2022). Monkeypox emergence shows immunopathogenesis and indicates immune evasions and antibody response, blood cell and granulocyte release, cytokines storm, and management of inflammatory events. Hence, this important virus has become another important concern for policymakers and healthcare providers and it has been assumed that another epidemic of the next level may occur if Monkeypox disease is not managed or treated in the early stages of detection. So, there is an urgent need to develop potential medicine that could inhibit Monkeypox viral infections and protect the globe from upcoming emerging epidemics.

Pinocembrin (5,7-dihydroxy flavanone) is a traditional chemical from the flavonoid group that has been known for its multifunctional properties (Rasul, 2013). So, it has been assumed that repurposing or modification of the functional group of Pinocembrin could produce better efficacy against viral pathogens such as Monkeypox. Therefore, based on a traditional finding of the parent compound Pinocembrin, the different functional group has substituted for the design of its derivatives, and *in silico* drug design approaches have been applied to confer their binding potential with Monekypox protein.

2. Materials and methods

The current study has been designed to get detailed investigations of the newly designed Pinocembrin compound derivatives to screen out the potential inhibitors against Monkeypox diseases, using Monkeypox virus protein. The step-wise methods are presented as follows.

2.1. Ligand preparation

The parent compound was Pinocembrin, an antiviral drug against the common viral threat in society. Its 2D and 3D structure was retrieved from the PubChem database (Kim, 2016) having identifier 68071. Derivatives of the parent compounds were designed by the addition/removal of functional groups in their structures and were prepared in ChemDraw Software (Mendelsohn, 2004) (Fig. 1). The structure of each derivative was saved in PDB file format for further docking analysis.

2.2. Selection of target protein

An appropriate antiviral target, the Monkeypox virus protein [PDB ID: 4QWO] (Minasov, 2022) structure identified by Minasov and his team, is used for *In silico* analysis. Prepared receptor and ligands were subjected to protein–ligand molecular docking (MD) application.

2.3. Molecular docking (MD) and interactions analysis

MD is an appropriate *in silico* method for determining drug interactions with the targeted bounded pathogen or receptor molecule and clarifying the mechanism of small derivatives molecules. Ligand and protein structures having hydrogen bonds and no atomic clashes in their structures were subjected to PyRx and performed ligand-based drug design. In this case, PyRx software's AutoDock mode (version 0.8) (Dallakyan and Olson, 2015) was used to simulate the precise MD. Discovery Studio software (Studio, 2008) is used for the interaction analysis of bounded complex structures.

2.4. Molecular dynamics simulations

To acquire a deeper understanding of the protein and chemical entities docked complex at the atomic level, molecular dynamic simulation (MDS) is performed. The structural stability of the chemical entities bounded in the active binding site of the targeted viral protein structure is examined for potential implementation by selecting the best-docked complexes for the MDS analysis at 100 ns. There were three main parts to this research that all related to using MDS: i) the parameter files were set; ii) pre-processing was carried out; and iii), the simulations themselves were carried out.

Antechamber module, complicated libraries, and distinct MDS were fixed using chemical entities and macromolecule information; solvation is achieved at 12 with the aid of the Leap module. Resolution of intermolecular interactions was achieved with the use of a force field (ff14SB) (T.-S. Lee, 2020). By introducing Na + ions, we were able to satisfy the need for charge neutralization. Following energy minimization for the system's carbon alpha atoms, a full set was run until "a thousand steps" with a pragmatic scale of 5 Kcal/mol-A^2, and the same was done for non-heavy atoms, for 300 steps. Therefore, the NVT ensemble was described with Langevin dynamics (Izaguirre et al., 2001), and the SHAKE algorithm was used to constrain the bonds involved between hydrogen atoms and heavy atoms. CPPTRAJ was used to detect interactions between and among molecules, using an 8.0 Å... distance cutoff (Roe and Cheatham, 2013). Visual Molecular Dynamic (VMD) software (Humphrey et al., 1996) was used for molecular visualization and to gain insight into the molecular behavior of simulated molecules.

2.5. Binding free energy estimation

Amber 20 is employed to calculate the integrated and solvation-free energy of the protein responsible for Monkeypox. To establish a distinction between the interacting contacts and non-interacting contacts demonstrate solvated conformations of the reported potential targets. MM-PBSA calculations were carried out on enzyme/protein–ligand complexes using MDS for 100 ns. The abso-

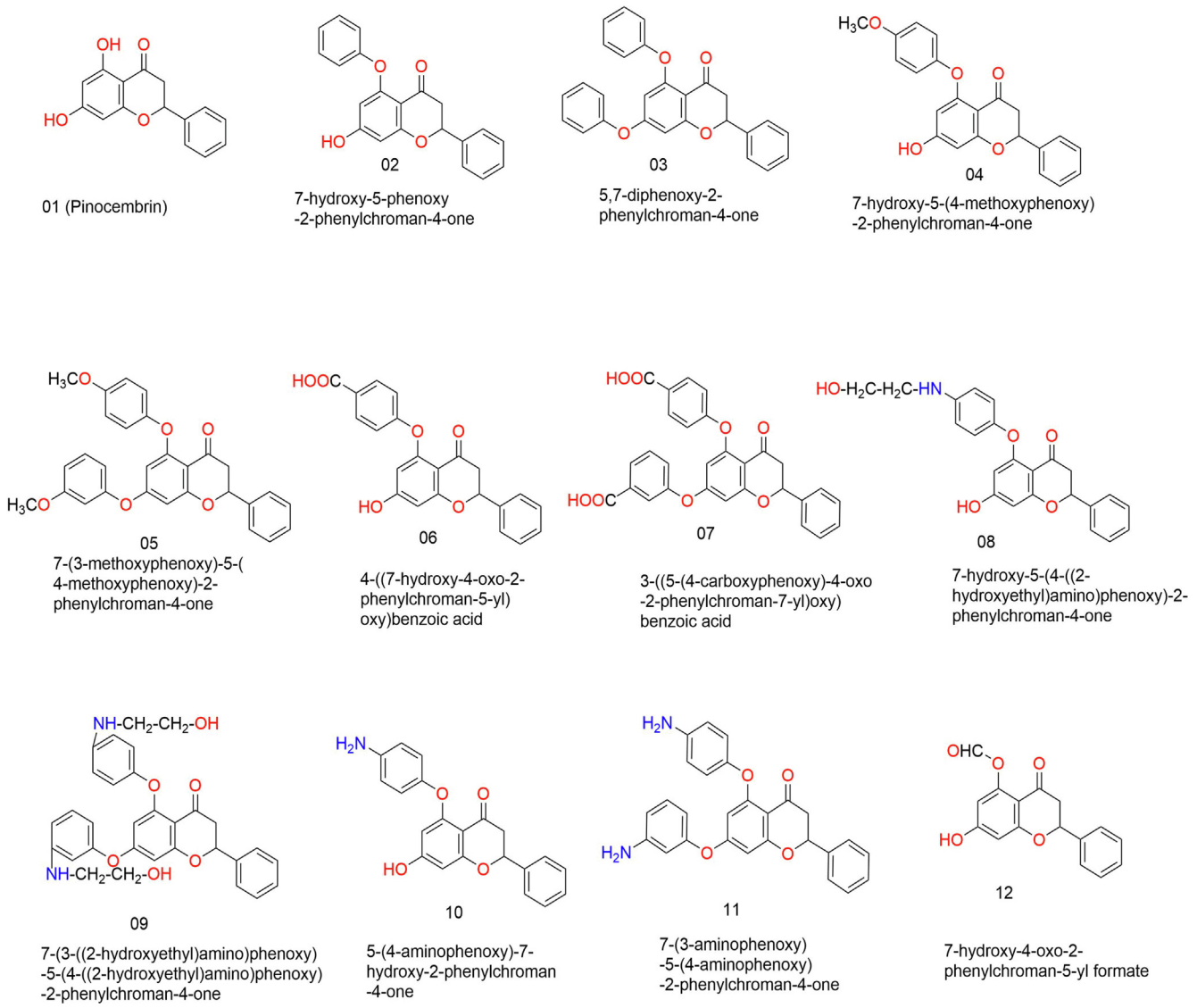

Fig. 1. Chemical structure of parent compound "Pinocembrin" and its derived compounds.

lute bond dissociation energy estimation is the sum of Gas-phase and solvation energies (Rastelli et al., 2010) (Tsai, 2020). The BFE may be decomposed scientifically using the regarding Equation (1).

$$\Delta G_{bind,solv} = \Delta G_{bind,vacuum} + \Delta G_{solv}, \textbf{target protien} - \textbf{ligand} - (\Delta G_{solv}, \textbf{ligand} + \Delta G_{solv}, \textbf{target protein}) \quad (1)$$

Using the solution of a single Poisson Boltzmann (PB) or Generalized Born (GB) formula, the solvation energy associated with the movement of substances from the gas phase to the solvent was calculated for all three MM system constraints. This means it will enhance the solvation phase's electrostatic function. Empirical terms for hydrophobic aids may be calculated in a similar fashion employing Equation (2).

$$\Delta G_{solv} = G_{electrostatic,\epsilon=80} - G_{electrostatic,\epsilon} = 1 + \Delta G_{hydrophobic}) \quad (2)$$

The calculation of the typical interaction energy between the chemical compound and receptor provides to ΔG vacuum, explained by Equation (3).

$$\Delta G_{vacuum} = \Delta E_{molecular\ mechanics} - T.\Delta S \quad (3)$$

2.6. ADMET profile calculations

With the exposure of structure-to-function analysis techniques, *in silico* Absorption, Distribution, Metabolism, Excretion, and Toxicity (ADMET) profile estimations have been investigated for the Pinocembrin-derivatives with the assistance of pkCSM (https://bisig.unimelb.edu.au/pkcsm/) to explain the molecular features. The SwissADME server (https://www.swissadme.ch/index.php) is used to calculate drug-likeness parameters.

2.7. PASS prediction

PASS server (https://www.pharmaexpert.ru/passonline/) has been applied to measure the PASS prediction score which is regarded as "Pa" and "Pi". Pa refers by probability to being active and Pi refers by probability to being inactive which ranges is 0.00–1.00; and, Pa + Pi ≠ 1 will never happen. Antiviral, antifungal, antibacterial, and antidiabetic activity has been calculated for the selected Pinocembrin derivatives.

3. Results

The structural modification, such as side chain, or functional groups modification applied to the parent compound "Pinocembrin" and derived 11 compound structures that are displayed in Fig. 1**,** used for molecular modeling and binding stability calculations. The advent of the microorganism Monkeypox virus produces a novel infectious disease and becomes a threat to human lives (Chadha et al., 2022). So, the *in silico* repurposing technique used in this research is the need for the development or shortlisting of potential antiviral drugs in a short time.

3.1. Molecular docking and interactions analysis

MD is an appropriate method used for the determination of drug interactions with the significant residues of targeted protein (Clark, 2006). Monkeypox virus protein three-dimensional structure (PDB ID: 4QWO) and ligands pdb structure files were subjected to PyRx software using the AutoDock Vina module and retrieve the best binding pose of selected compounds to estimate a significant number of interactions with protein residues (Dallakyan and Olson, 2015). Default settings were applied during MD, and a blind docking technique was applied for this study.

Table 1
Calculated docking affinity of selected ligands against viral protein.

Ligands	4QWO –Monkeypox Virus
	Binding affinity (kcal/mol)
01	−7.5
02	−8.8
03	−9.2
04	−8.5
05	−9.0
06	−9.0
07	−10.3
08	−8.5
09	−9.0
10	−9.0
11	−9.6
12	−7.0

The calculated docking affinity of selected ligands against the viral protein is enlisted in Table 1. Binding affinities have been calculated in the range of −7 to −10 Kcal/mol when docked selected ligands with 4QWO-Monkeypox virus protein, it seems that selected derivatives could be effective agents against the Monkeypox disease due to best-docked score and good binding interactions with the residues of selected protein.

Best bounded conformations were saved and binding interactions of protein-derivative docked complexes were generated by Biovia Discovery Studio 2020 (Dey et al., 2022), shown in Figs. 2, and 3**.** Each color presents different kinds of binding interactions among atoms of ligands and residues of active binding sites of selected protein, such as green colored circles representing van der Waal contacts and hydrogen bonds, while purple circles represent alkyl and Pi-alkyl interactions, and so on. Molecular docking results of the top-1 and top-2 dock score compounds with target protein are summarized in Table 2.

3.2. Molecular dynamic simulation (MDS)

Based on static interacting contacts of best-bounded protein-derivative complex, by keeping the macromolecule rigid and derivatives (ligands) as flexible, two docked complexes of derivatives **07,** and **11** were subjected to MDS for 100 ns, to understand the stability and flexibility of the binding contacts with residues of selected protein under physiological conditions and hence the potential complexes retrieved impressive results. The stability of the protein and selected derivative compound was estimated, the superimposed macromolecular structures at 0 ns with 100 ns were studied carefully, and estimated RMSD values of the difference for protein complexes with **07** and **11** were calculated as 1.2 and 1.3, respectively, and that infers the protein complex may undergo minor conformational changes at the following selected temperature.

The superimpose structure of derivative compound-**07** pose at 0 ns with the pose at 100 ns, RMSD value for the stabilized complex is 1.2427 Å as shown in Fig. 4. It can be seen a slight movement in the ligand binding position. Since the compound remained attached within the binding cavity, therefore, it can be assumed that this movement is the result of achieving a more stable and

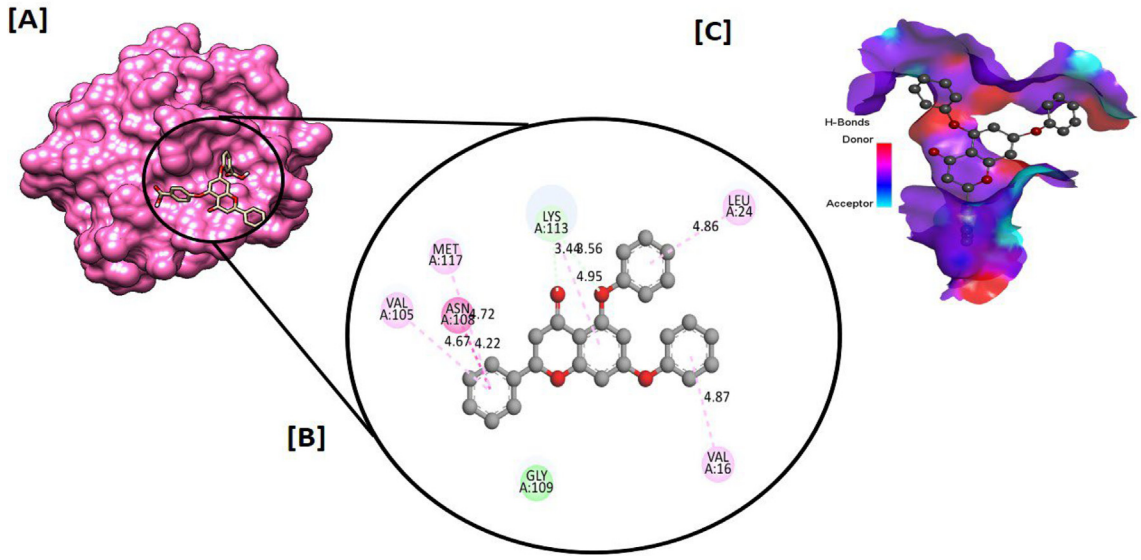

Fig. 2. Docking interactions between the proposed derivative (O7) and Monkeypox virus protein [PDB ID: 4QWO] with the best dock score in Kcal/mol presenting the best bounded-conformation within an active binding site [A], Two-dimensional plot presenting binding elements [B], and hydrogen bonding capacity of the residues in active binding site is shown in [C].

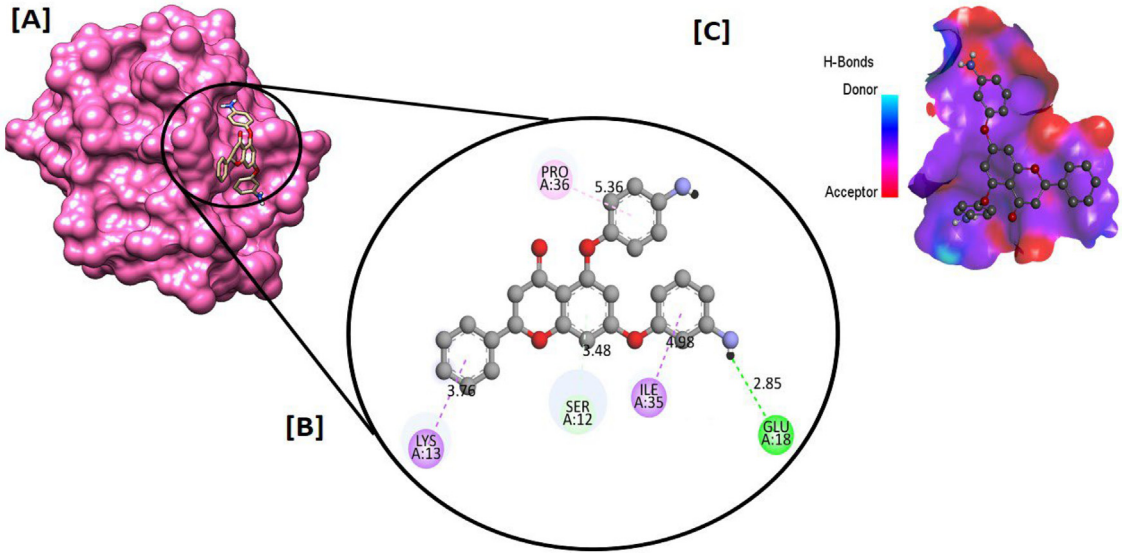

Fig. 3. Docking interactions between the proposed derivative (11) and Monkeypox virus protein [PDB ID: 4QWO] with the best dock score in Kcal/mol presenting the best-bounded conformation within an active binding site [A], Two-dimensional plot presenting binding elements [B], and hydrogen bonding capacity of the residues in active binding site is shown in [C].

Table 2
Molecular docking outcomes for top-scored PDB ID: 4QWO–Monkeypox virus protein.

Ligands #	Ligands names	Dock score (Kcal/mol)	Functional groups involved in binding interactions	Binding interactions	
				Interacting residues	Bond distances (Å)
07	3-((5-(4-carboxyphenoxy)-4-oxo-2-phenylchroman-7-yl)oxy)benzoic acid	−10.3	Benzene ring, and carboxylic group	HIS-5	2.88
				SER-12	3.49
				LYS-13	4.39
				PHE-17	2.74
				ILE-35	3.84
				ILE-35	3.90
				PRO-36	5.34
11	7-(3-aminophenoxy)-5-(4-aminophenoxy)-2-phenylchroman-4-one	−9.6	Benzene ring, and NH_2 group	SER-12	3.48
				LYS-13	3.76
				GLU-18	2.85
				ILE-35	3.73
				ILE-35	3.99
				ILE-35	3.78
				PRO-36	5.36

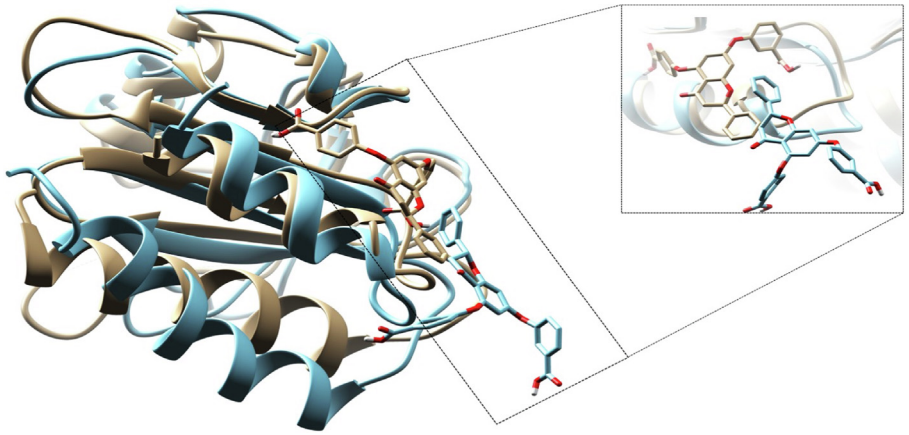

Fig. 4. Superimposition of derivative compound "3-((5-(4-carboxyphenoxy)-4-oxo-2-phenylchroman-7-yl) oxy) benzoic acid" bounded with 4QWO-Monkeypox protein from 0 to 100 ns. RMSD value for stabilized complex is 1.2427 Å, protein and derivative compound at 0 ns is presented in brown, while at 100 ns is presented in blue color.

strong binding pose. This statement can be supported with RMSD analysis of MD simulation trajectories (Fig. 5A). A complete trajectory analysis for compound **07** is displayed in Fig. 5. RMSD graph shows very few rising peaks at the start of the simulation and remains stable from 45 ns to 100 ns. The average RMSD was noted as 2.927256 (Fig. 5A). Further, protein residues showed substantial fluctuations throughout the simulation. This can be the effect of bounded compounds on protein conformations. An average RMSF was noted as 1.099408 (Fig. 5B). Hydrogen bond analysis also shows a firm binding between the compound and the target protein **(**Fig. 5c). Additionally, SASA analysis also indicates the stability of the system (Fig. 5F).

Superimposed studies of derived compound **11** at 0 ns and 100 ns showed no major changes in the binding pose with an RMSD value of 1.279 Å (Fig. 6). Further, the trajectories analysis of compound **11** elucidated the complex stability (Fig. 7**)**. No major fluctuations were recorded in RMSD and RMSF analysis with average values of 2.074399 and 1.141168, respectively. Additionally, hydrogen bond and SASA analysis also support the firm and stable binding of compound 11 within the binding pocket of the receptor.

3.3. Binding free energy estimation

The binding free energy (BFE) is estimated by using the famous energy modules; PBSA and GBSA, and the results estimated sup-

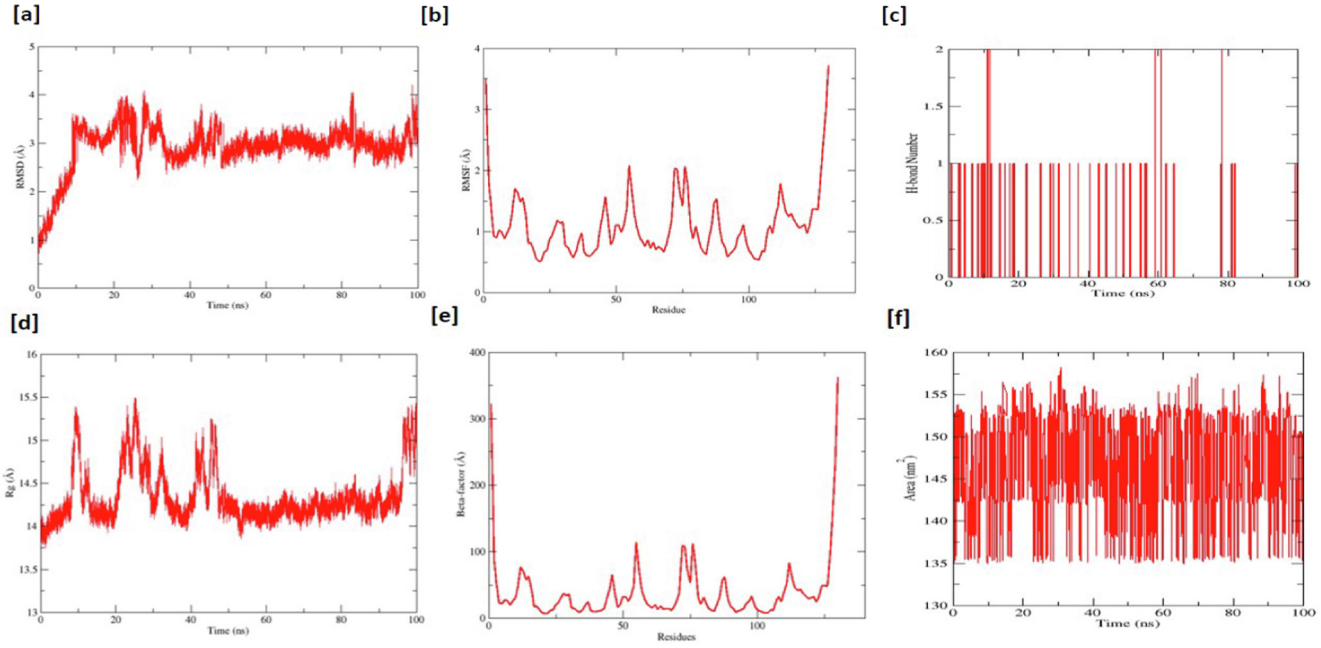

Fig. 5. RMSD value of Monkeypox protein with derivative compound "3-((5-(4-carboxyphenoxy)-4-oxo-2-phenylchroman-7-yl)oxy)benzoic acid" complex [a] shown in Angstrom (Å) (Y-axis) and the variation of poses through time in nanoseconds (ns) (X-axis). RMSF of Monkeypox macromolecule [b] in-unit Angstrom (Å) (Y-axis) and index of the residue throughout 0–100 ns (Y-axis). Hydrogen bonds of derivative compound till 100 ns [d]. Considered hydrogen bonds (Y-axis) and variation to timespan during MDS (X-axis). Rg of macromolecule and derivative compound complex [d] (Y-axis) in-unit Angstrom (Å), and variation of bonded conformation throughout MDS (Y-axis). A beta factor of Monkeypox macromolecule [e] (Y-axis) in-unit Angstrom (Å) and the index of the residue until 100 ns (X-axis). While SASA of Monkeypox macromolecule presents backbone calculations [f]. Thermodynamically occurring changes in Monkeypox and derivative compound complex surface area are shown in unit nanometers square (nm2) (Å) (Y-axis) and the macromolecule residues steadiness is explained in time during 0–100 ns (X-axis).

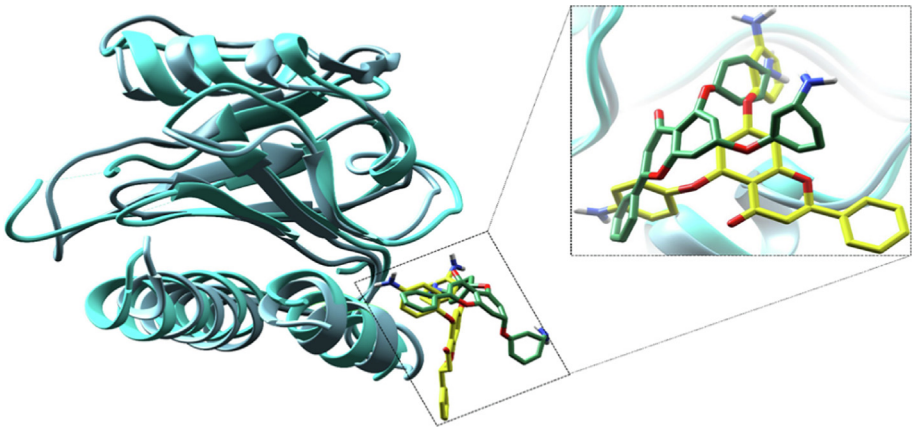

Fig. 6. Superimposition of derivative compound "7-(3-aminophenoxy)-5-(4-aminophenoxy)-2-phenylchroman-4-one" bounded with 4QWO –Monkeypox protein from 0 ns and 100 ns. RMSD value for stabilized complex is 1.279 Å, and the protein is in cyan, the derivative compound in yellow is presented at 0 ns, while at 100 ns, and protein is presented in dark grey, and the derivative compound is in dark green color.

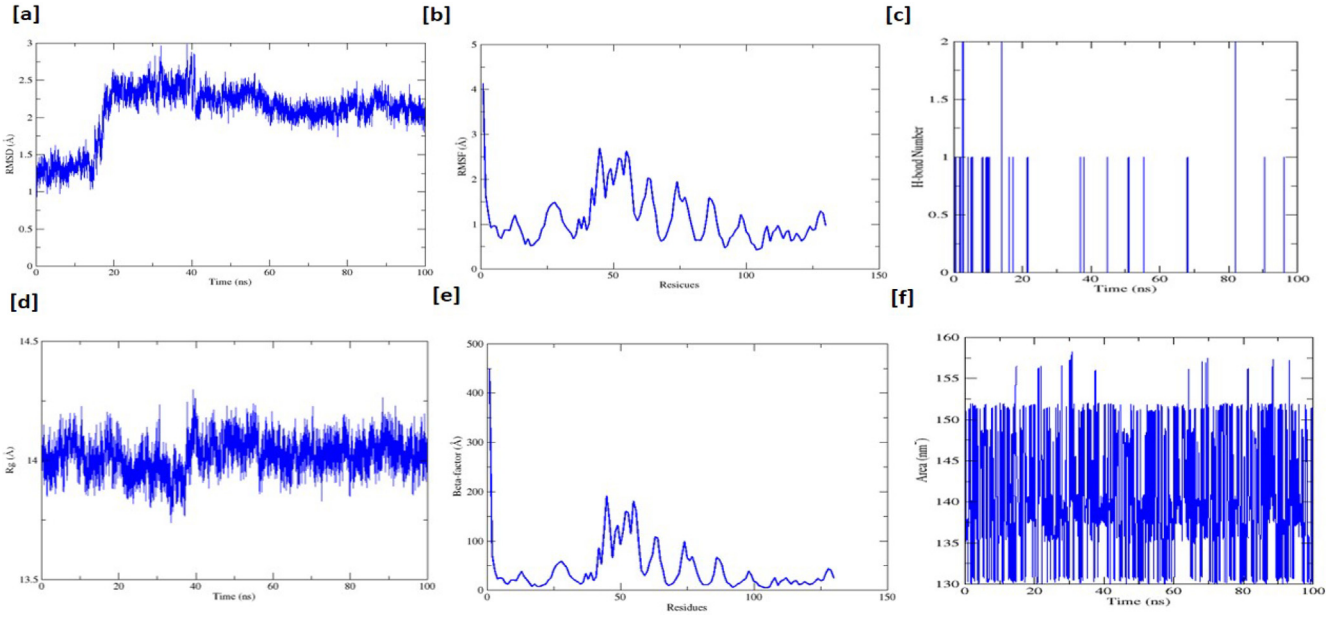

Fig. 7. RMSD value of Monkeypox protein with derivative compound "7-(3-aminophenoxy)-5-(4-aminophenoxy)-2-phenylchroman-4-one" complex [a] shown in Angstrom (Å) (Y-axis) and the variation of poses through time in nanoseconds (ns) (X-axis). RMSF of Monkeypox macromolecule [b] in-unit Angstrom (Å) (Y-axis) and index of the residue throughout 0–100 ns (Y-axis). Hydrogen bonds of derivative compound till 100 ns [d]. Considered hydrogen bonds (Y-axis) and variation to timespan during MDS (X-axis). Rg of macromolecule and derivative compound complex [d] (Y-axis) in-unit Angstrom (Å), and variation of bonded conformation throughout MDS (Y-axis). A beta factor of Monkeypox macromolecule [e] (Y-axis) in-unit Angstrom (Å) and the index of the residue until 100 ns (X-axis). While SASA of Monkeypox macromolecule presents backbone calculations [f]. Thermodynamically occurring changes in Monkeypox protein and derivative compound complex surface area are shown in unit nanometers square (nm2) (Å) (Y-axis) and the macromolecule residues steadiness explained in time during 0–100 ns (X-axis).

port the analysis of protein folding and stability as explained in the previous literature (Shah et al., 2022). The total energy of the selected protein and derivative-complex trailed with the generalized surface area Born (MM/GBSA) framework the well-organized estimations destitute of any loss concerning accuracy and Poisson Boltzmann (MM/PBSA) modeling (Genheden and Ryde, 2015). It can be noteworthy for the representation of the potent anti-viral macromolecule [PDB ID: 4QWO] with chemical derivatives (**7**, and **11**) complex in the pure water.

Delta E total differences studied by the MM/GBSA and MM/PBSA models for the ligands docked best with 4QWO, such as for (**07)** derivative complex is −7.5249 kcal and −5.5637 kcal/mol; and for the MM/PBSA model (**11)** derivative complex is −24.9043 kcal and −19.7435 kcal/mol respectively. For molecular mechanics' energy constraints, a clear effect has been examined from the gas-phase energy when studying the contributions of solvation energy. In the MM/GBSA model of the (**07)** derivative complex, the ΔG gas energy was maintained at at 79.9720 kcal/mol, and in the MM/PBSA model, the same energy parameters were maintained at 79.9720 kcal/mol, and the ΔG solv energy maintained at −87.4969 kcal/mol, for MM/GBSA model maintained at −85.5357 kcal/mol, for MM/PBSA model, similarly for (**11)** derivative complex, the ΔG gas energy maintained at 33.3448 kcal/mol in the MM/GBSA and MM/PBSA models, and ΔG solv energy maintained at −58.2491 kcal/mol and for MM/GBSA model maintained at −53.0882 kcal/mol.

The electrostatic forces play a role in the stability of the complex, and the system estimated by MM forces field in PBSA/GBSA is in the range of total premeditated energy calculated as 93.6571Kcal/mol for (**07)** derivative complex and 59.9666 Kcal/-mol for (**11)** derivative complex. Similarly, the Van der Waals forces are also estimated from MM associated with the system stability maintained at −13.6850 Kcal/mol for the (**07)** derivative complex and −26.6218 Kcal/mol for (**11)** derivative complex. The surface area energy highlighted as ESURF computed in the MM/GBSA model is maintained at −2.0844 Kcal/mol for (**07)** derivative complex, and −3.2400 Kcal/mol for (**11)** derivative complex, The values of ENPOLAR and EDISPER, maintained at −1.7625 kcal/mol and Zero kcal/mol for (**07)** derivative complex, and ENPOLAR maintained at −2.3513 Kcal/mol for (**11)** derivative complex. For the docked complex, the electrostatic energy impact, EGB, and EPB to the ΔG solv were counted as non-favorable results in MM/GBSA solv energy (Table 3).

3.4. ADMET profile calculations

Molecular specifications such as membrane permeability and bioavailability of drug candidates are dependent on some core aspects of derivative compounds. These characteristics include the molecular weight (MW), the partition coefficient (logP), and the number of hydrogen bond acceptors/donors that are affiliated with the "rule of five" proposed by Lipinski. In Table 4, the molecular weight ranges for the best two derivative compounds are less than 500 Dalton, the number of rotatable bonds 05 and 07, hydrogen bond acceptor are 04 and 08, hydrogen bond donor are 02, topological polar surface area, less than 120 $Å^2$ and consensus Log Po/w is 4.20 and 4.36 which all are within ranges of Lipinski five rule and presents data of the pinocembrin derivatives (**07,** and **11**). If a substance's bioavailability score is more than 0.50 is considered to have the potential to participate in biochemical functions. The bioavailability score found for the mentioned compounds is 0.55.

pkCSM online tool used to calculate numerous parameters such as water solubility (Log S), Caco-2 permeability, intestinal absorption (human), the volume of distribution (human) (log L/kg), BBB permeability, CYP450 1A2 inhibitor, CYP450 2C9 inhibitor, total clearance (ml/min/kg), and renal OCT2 substrate. Pinocembrin derivatives, **07** and **11** are water-soluble as scored −2.909, and −3.909 which represents they are highly soluble in an aqueous system. The Caco-2 permeability range has been found 0.35 mole-

Table 3
Binding free energies of the Monkeypox virus protein and selected potential derivatives complexes.

MM/GBSA model				MM/PBSA model			
Energy Components	**Average**	**Std. Dev**	**Std. Err. of Mean**	**Energy Components**	**Average**	**Std. Dev**	**Std. Err. of Mean**
Ligand O7 – Monkey-Pox protein [PDB ID: 4QWO] complex							
VDWAALS	−13.6850	1.6332	0.1826	VDWAALS	−13.6850	1.6332	0.1826
EEL	93.6571	12.3659	1.3825	EEL	93.6571	12.3659	1.3825
EGB	−85.4126	11.9144	1.3321	EPB	−83.7732	12.3688	1.3829
ESURF	−2.0844	0.1368	0.1368	ENPOLAR	−1.7625	0.1022	0.0114
				EDISPER	0.0000	0.0000	0.0000
ΔG gas	79.9720	11.6695	1.3047	ΔG gas	79.9720	11.6695	1.3047
ΔG solv	−87.4969	11.9134	1.3320	ΔG solv	−85.5357	12.3681	1.3828
ΔTOTAL	−7.5249	1.1615	0.1299	ΔTOTAL	−5.5637	1.3830	0.1546
Ligand 11 – Monkey-Pox protein [PDB ID: 4QWO] complex							
VDWAALS	−26.6218	2.3404	0.2340	VDWAALS	−26.6218	2.3404	0.2340
EEL	59.9666	8.8502	0.8850	EEL	59.9666	8.8502	0.8850
EGB	−55.0091	7.4694	0.7469	EPB	−50.7369	6.8816	0.6882
ESURF	−3.2400	0.1422	0.0142	ENPOLAR	−2.3513	0.0729	0.0073
				EDISPER	0.0000	0.0000	0.0000
ΔG gas	33.3448	8.5605	0.8560	ΔG gas	33.3448	8.5605	0.8560
ΔG solv	−58.2491	7.4463	0.7446	ΔG solv	−53.0882	6.8868	0.6887
ΔTOTAL	−24.9043	2.4559	0.2456	ΔTOTAL	−19.7435	4.0608	0.4061

Table 4
Summary of pharmacokinetic profile estimated for selected two best derivatives.

Properties	**O7**	**11**
MW	496.46	438.47
NBR	7	5
HBA	8	4
HBD	2	2
TPSA (Å)	119.36	96.80
Consensus Log Po/w	4.36	4.20
Bioavailability Score	0.56	0.55
Water Solubility Log S	−2.909	−3.909
Caco-2 Permeability (10^{-6} cm/s)	0.356	0.357
Intestinal absorption (human) (%)	64.689	100
BBB permeability	No	No
CYP4501A2 inhibitor	No	No
CYP4502C9 inhibitor	Yes	Yes
Renal OCT2 substrate	No	No
AMES toxicity	No	No
Max. tolerated dose (human) mg/kg/day	0.495	0.424
Oral Rat Acute Toxicity (LD50) (mol/kg)	3.334	3.219
Oral Rat Chronic Toxicity (mg/kg/day)	0.984	0.675

cules with lower than 30% has been considered a moderately low absorbance rate (Pires et al., 2015). Both candidates have good intestinal absorption, **07**, and **11** have found 64.689% and 100%. Both candidates can be potential CYP4502C9 inhibitors. The aquatic and non-aquatic toxicity ensure the quality and safety profile of a drug candidate for human use and environmental exposure. The AMES toxicity, max tolerated dose, oral rat acute toxicity (LD50), hepatotoxicity, and skin sensitization have been predicted well. The max tolerated dose range has been obtained as 0.4 mg/kg/day. The oral rat acute toxicity (LD50) was gained 3 mol/kg and finally, the oral rat chronic toxicity level was predicated at 0.9 mg/kg/day and 0.6 mg/kg/day. The results indicated that the predicted candidates could be safer drugs.

3.5. Evaluation of antiviral efficacy (PASS Prediction) activity

The antimicrobial spectrum was also anticipated by using the virtual server PASS for two derivatives **07** and **11**. Both candidates were selected based on the maximum docking score. The findings of the PASS test are shown in Table 5 and are written in the form of Pa and Pi. These designed derivatives exhibited antibacterial activity, antiviral, and antifungal activity. The effectiveness of these derivative compounds against viral pathogens was much higher

Table 5
Pass prediction against pathogenic efficacy of selected best three derivatives.

Ligand No	Antiviral (Rhinovirus)		Antibacterial		Antifungal	
	Pa	**Pi**	**Pa**	**Pi**	**Pa**	**Pi**
07	0.603	0.006	0.363	0.040	0.503	0.030
11	0.534	0.015	0.292	0.063	0.448	0.040

than their effectiveness against bacteria, and fungal infections. So, due to a greater Pa score of selected derivatives against antiviral activity, the Monkeypox virus potential could be tested in the lab by further analysis.

4. Discussion

The parent compound "Pinocembrin" is a medicinal compound that has been investigated for antiviral therapies (Rasul, 2013). The Pinocembrin compound is an active inhibitor of the Zika virus, and its activity has been demonstrated in human placental JEG-3 cells (IC50 = 17.4 μM) (J. Le Lee et al., 2019). Therefore it is thought to be active for other viruses, In this study, based on the structure modification technique using different functional groups, we have designed derivatives/analogs of the Pinocembrin compound, modifications are clearly shown in Fig. 1.

Computational screening-based drug design investigations of designed derivatives of Pinocembrin for the identification of potent drugs for Monkeypox disease have been conducted very carefully, each result has demonstrated well to explain its importance.

Molecular modeling techniques such as MD and MDS have demonstrated the interaction with significant residues and stability of the docked derivatives structures with selected protein, and a very important aspect is binding energies calculations, that's highlighted in Tables 1–3. With the Monkey pox protein (4QWO), HIS-5, SER-12, PHE-17, ILE-35, PRO-36, and LYS-13 residues make contacts with 3-((5-(4-carboxyphenoxy)-4-oxo-2-phenylchroman-7-yl)oxy)benzoic acid (**07**) ligand, SER-12, LYS-13, GLU-18, ILE-35, ILE-35, and PRO-36 residues make contacts with 7-(3-aminophenoxy)-5-(4-aminophenoxy)-2-phenylchroman-4-one (**11**) ligand (Figs. 2 and 3). The best-bounded conformations were further subjected to the deep-down analysis of MD simulations. Selected chemical entities showed high stability in MD simulations with a force field (ff14SB). Results demonstrated the number of

hydrophobic and hydrogen bond contacts as potential contributors of docked-ligand stability in the best-bounded conformation, explaining the drug molecules' stability. Following the *in silico* research, it is considered that obtained results signify the conformational stability of the bounded complex because of minor fluctuations, hence further explaining the evidence of MD simulation results at 100 ns (Figs. 4-7), which highlighted the selected three potential derivatives; 3-((5-(4-carboxyphenoxy)-4-oxo-2-phenyl chroman-7-yl)oxy)benzoic acid **(07),** and 7-(3-aminophenoxy)-5-(4-aminophenoxy)-2-phenylchroman-4-one **(11)** are the best fit within the structural conformation of 4QWO. A complete trajectory analysis for derivative compound (**07**) is demonstrated in Fig. 5. RMSD graph shows very few rising peaks at the start of the simulation and remains stable from 45 ns to 100 ns. The average RMSD was noted as 2.927256 Å and an average RMSF was noted as 1.099408 Å (Fig. 5a and 5b). Hydrogen bond analysis also shows a firm binding between the compound and the target protein, average valued noted as 0.072927 (Fig. 5c). The average value of Rg noted from the graph is 14.34604 Å (Fig. 5d), Additionally, SASA analysis also indicates the stability of the system (Fig. 5e), average value noted as 14.34604. Beta-factor was also calculated defining the displacement of atoms during the MDS intervals depending upon the RMSD fluctuations, the average beta-factor value was noted as 39.01999 Å for the derivative compound (**07**) **(**Fig. 5f**).** Likewise, the same parameters were noted for the derivative compound **(11), the** average RMSD noted was 2.074399 Å, showing minor fluctuations in the graph, an average RMSF noted was 1.141168 Å (Fig. 7a and 11b), average hydrogen bond number calculated is 0.33966 (Fig. 7c) refers to the protein pockets hydrophobic characteristics, Average Rg value noted as 14.01982 Å and shown in Fig. 7d, Average SASA value noted close to140.8129 and presented in Fig. 7e and average beta-factor noted as 43.16434 Å (Fig. 7f). The stability of the virtual hit molecules (**07** and **11**) with the pathogenic receptor protein is important, hence the average values for each MDS analysis were noted to determine the fluctuation of results concerning binding stability with the target, it is observed that small conformational changes found in the start of MDS and overall results are good and stable structures. During MDS the noted fluctuations highlighted the presence of loops in the structures. Further experimental analysis is required to validate the computational hypothetical results to confirm the inhibitory character against the Monkeypox disease.

ADMET profile estimations and Pass predictions for potential virtual hit molecules (**07** and **11**) were additionally conducted to evaluate the drug-likeness activity of the selected derivative compounds, Each compound has presented acceptable chemical and physical properties (Table 4), and it estimated that the effectiveness of these selected potential hits/derivatives against viral pathogens was much higher than their effectiveness for bacterial, and fungal infections (Table 5). Hence this *In silico* study could be a roadmap to propose Monkeypox antiviral drugs with the best bounded aspects within enzyme pocket as well as good medicinal chemistry and bioavailability estimations.

5. Conclusions

The Monkeypox virus has affected a large number of patients globally. However, there has been no effective drug for the inhibition of several viral diseases. Therefore, computational approaches have been conducted to design effective derivatives by structural modification in the Pinocembrin structure. Further, MD simulation indicates a firm and stable binding of derived compounds within the binding pocket of the receptor. Additionally, MMPBSA/GBSA-based energy calculations further supported the potential of compound activity against the receptor. After overall investigation, it has been estimated that all the derived compounds possess good binding affinities with Monkeypox protein that lie in the range of 7.00 to –10.3 kcal/mole. The derived compounds (**07** and **11**) also presented good pharmacokinetic profiles with minor violations. The drug-likeness rules for derived compounds are satisfied. Further experimental analyses are recommended to be performed in the wet lab to validate the computational hypothetical results to confirm the inhibitory character against the Monkeypox disease. Pinocembrin-derived compounds (**07** and **11**) could be potential suppressors of Monkeypox in Humans.

Funding

This work was funded by Princess Nourah bint Abdulrahman University Researchers Supporting Project number (PNURSP2023R342), Princess Nourah bint Abdulrahman University, Riyadh, Saudi Arabia. This work was funded by the Researchers Supporting Project number (RSPD2023R628), King Saud University, Riyadh, Saudi Arabia.

CRediT authorship contribution statement

Shopnil Akash: Conceptualization, Writing – original draft, Data curation, Formal analysis. **Shabana Bibi:** Conceptualization, Project administration, Supervision, Visualization, Writing – review & editing, Writing – original draft, Validation, Formal analysis, Software, Data curation, Methodology. **Qudsia Yousafi:** Validation, Writing – review & editing, Writing – original draft. **Awais Ihsan:** Writing – review & editing. **Riaz Mustafa:** Writing – review & editing. **Umar Farooq:** Writing – review & editing. **Atul Kabra:** Methodology, Visualization, Writing – review & editing, Writing – original draft. **Mohammad M. Alanazi:** Writing – review & editing. **Ashwag S. Alanazi:** Writing – review & editing. **Omkulthom Al Kamaly:** Writing – review & editing.

Declaration of Competing Interest

The authors declare that they have no known competing financial interests or personal relationships that could have appeared to influence the work reported in this paper.

Acknowledgments

The authors extend their appreciation to Princess Nourah bint Abdulrahman University Researchers Supporting Project number (PNURSP2023R342), Princess Nourah bint Abdulrahman University, Riyadh, Saudi Arabia. The authors extend their appreciation to the Researchers Supporting Project number (RSPD2023R628), King Saud University, Riyadh, Saudi Arabia.

References

Akash, S., Rahman, M.M., Islam, M.R., Sharma, R., 2022. Emerging global concern of langya henipavirus: pathogenicity, virulence, genomic features, and future perspectives. J. Med. Virol.

Billioux, B.J., Mbaya, O.T., Sejvar, J., Nath, A., 2022. Neurologic complications of smallpox and monkeypox: a review. JAMA Neurol.

Boopathi, S., Poma, A.B., Kolandaivel, P., 2020. Novel 2019 coronavirus structure, mechanism of action, antiviral drug promises and rule out against its treatment. J. Biomol. Struct. Dyn.

Ciotti, M. et al., 2020. The COVID-19 pandemic. Crit. Rev. Clin. Lab. Sci. 57 (6), 365–388.

Clark, D.E., 2006. What has computer-aided molecular design ever done for drug discovery? Expert Opin. Drug Discov. 1 (2), 103–110.

Dallakyan, S., Olson, A.J., 2015. Small-molecule library screening by docking with PyRx. In: Chemical Biology. Springer, pp. 243–250.

Frenkel, L.D., Bellanti, J.A., 2022. Monkeypox viral infection and disease: a challenge for the allergist-immunologist. Allergy Asthma Proc.

Hoffmann, C. et al., 2022. clinical characteristics of monkeypox virus infections among men with and without HIV: a large outbreak cohort in Germany. HIV Med.
Howard, C.R., Fletcher, N.F., 2012. Emerging virus diseases: can we ever expect the unexpected? Emerging Microbes Infect. 1 (1), 1–9.
Hutchinson, E.C., 2018. Influenza virus. Trends Microbiol. 26 (9), 809–810.
Hutson, C.L. et al., 2015. Laboratory investigations of African pouched rats (Cricetomys Gambianus) as a potential reservoir host species for monkeypox virus. PLoS Negl. Trop. Dis. 9 (10), e0004013.
Izaguirre, J.A., Catarello, D.P., Wozniak, J.M., Skeel, R.D., 2001. Langevin stabilization of molecular dynamics. J. Chem. Phys. 114 (5), 2090–2208.
Jones, K.E. et al., 2008. Global trends in emerging infectious diseases. Nature 451 (7181), 990–993.
Kim, S. et al., 2016. PubChem substance and compound databases. Nucleic Acids Res. 44 (D1), D1202–D1213.
Lee, T.-S. et al., 2020. Alchemical binding free energy calculations in AMBER20: advances and best practices for drug discovery. J. Chem. Inf. Model. 60 (11), 5595–5623.
Lee, L.e., Jia, M.W., Loe, C., Lee, R.C.H., Chu, J.J.H., 2019. Antiviral activity of pinocembrin against zika virus replication. Antiviral Res. 167, 13–24.
Mahase, E., 2022. Seven Monkeypox Cases Are Confirmed in England.
Malvy, D. et al., 2019. Ebola virus disease. Lancet 393 (10174), 936–948.
Mauldin, M.R. et al., 2022. Exportation of monkeypox virus from the african continent. J Infect Dis 225 (8), 1367–1376.
Mendelsohn, L.D., 2004. ChemDraw 8 ultra, windows and macintosh versions. J. Chem. Inf. Comput. Sci. 44 (6), 2225–2226.
Minasov, G. et al., 2022. Structure of the monkeypox virus profilin-like protein A42R reveals potential functional differences from cellular profilins. Acta Crystall. Sect. F: Struct. Biol. Commun. 78 (10), 371–437.
Mourya, D.T. et al., 2019. Emerging/re-emerging viral diseases new viruses on the indian horizon. Indian J. Med. Res. 149 (4), 447.
Rastelli, G., Del Rio, A., Degliesposti, G., Sgobba, M., 2010. Fast and accurate predictions of binding free energies using MM-PBSA and MM-GBSA. J. Comput. Chem. 31 (4), 797–810.
Rasul, A. et al., 2013. Pinocembrin: a novel natural compound with versatile pharmacological and biological activities. BioMed Res. Int. 2013.
Ross, T.M., 2010. Dengue virus. Clin. Lab. Med. 30 (1), 149–160.
Sale, T.A., Melski, J.W., Stratman, E.J., 2006. Monkeypox: an epidemiologic and clinical comparison of African and US disease. J. Am. Acad. Dermatol. 55 (3), 478–481.
Sklenovska, N., Van Ranst, M., 2018. Emergence of monkeypox as the most important orthopoxvirus infection in humans. Front. Public Health 6, 241.
Studio, D., 2008. Discovery studio. Accelrys [2.1].
Thornhill, J.P. et al., 2022. Monkeypox virus infection in humans across 16 countries—April–June 2022. N. Engl. J. Med. 387 (8), 679–691.
Tsai, H.-C. et al., 2020. Validation of free energy methods in AMBER. J. Chem. Inf. Model. 60 (11), 5296–5300.
Vaheri, A. et al., 2013. Uncovering the mysteries of hantavirus infections. Nat. Rev. Microbiol. 11 (8), 539–550.
von Magnus, P., Andersen, E.K., Petersen, K.B., Birch-Andersen, A., 1959. A pox-like disease in cynomolgus monkeys. Acta Pathol. Microbiol. Scand. 46 (2), 156–176.